fast DART
DATA, ANALYSIS, REVIEWS, TECHNIQUES E-JOURNAL

Biotechniques

Standardized Electrophysiological Approaches for CA1 Field Recordings: Insights into the AS Mouse Model

Melinda M Peters [1], Joseph E. Pick [2] and Edwin J. Weeber [3*]

[1]Independent Researcher, PA, USA
[2]Independent Researcher, NY, USA
[3]Foundation for Angelman Syndrome Therapeutics, San Antonio, TX, USA
[*]Corresponding author; edwin.weeber@cureangelman.org

Article History
Submitted: September 18, 2025 Accepted: October 24, 2025 Published: November 1, 2025

Abstract

The hippocampal CA3/CA1 Schaffer collateral pathway provides a lamina-resolved and highly reproducible synaptic pathway for quantifying synaptic transmission and plasticity in acute rodent brain slices. This paper consolidates best practices for CA1 field electrophysiology and links them to disease-relevant readouts in Angelman syndrome (AS) models. We detail a rigorously controlled pipeline spanning sucrose-based, low-Ca^{2+}/high-Mg^{2+} cutting solutions; staged recovery from ice-cold to warmed (30–32 °C) artificial cerebrospinal fluid (ACSF); strict management of bicarbonate buffering to prevent divalent precipitation; and recording parameters that yield clean, minimally filtered field excitatory post-synaptic potentials (EPSPs). Quantification emphasizes the initial field excitatory post-synaptic potential (fEPSP) slope measured within a fixed, pre-registered window, normalization to a stable baseline, and exclusion criteria that guard against artifacts. We outline how input–output curves, establish basal synaptic gain and the operating point for plasticity assays, and we compare induction paradigms-consisting of classical 100 Hz high frequency stimulation (HFS), theta-frequency and theta-burst stimulation, and ultra-high-frequency stimulation. Applying this framework to AS mouse and rat models, we summarize how electrophysiology discriminates a shifted induction threshold from a true capacity deficit requiring restoration of downstream expression mechanisms or Ube3a function. The approach delivers a mechanistically interpretable, quantitative biomarker for AS that is suitable for preclinical screening and for testing gene-targeted and synaptic-level therapies. Collectively, these standardized practices, spanning anatomy, solutions, data acquisition, and analysis, establish a reproducible framework and a translational lens for interpreting hippocampal LTP in AS and other neurodevelopmental disease models.

Keywords: Long-term potentiation, hippocampus, high frequency stimulation, animal models, synapse, synaptic function, synaptic plasticity.

Introduction

The hippocampal formation (dentate gyrus-CA3-CA1-subiculum) is both anatomically simple and exquisitely ordered, which is why it has been a standard of synaptic physiology for decades. Entorhinal cortex layer II neurons project via the perforant path to the dentate gyrus (DG), whose granule cells send mossy fibers to CA3 (terminating in

stratum lucidum) (Witter, 2007) (Amaral et al., 2007). CA3 pyramidal neurons then project to CA1 via the Schaffer collaterals (SCs), while a parallel "temporoammonic" input from entorhinal layer III reaches the distal apical tufts of CA1 in stratum lacunosum-moleculare (Remondes and Schuman, 2002). CA1 outputs to the subiculum and back to entorhinal cortex, completing the hippocampal–entorhinal loop that supports episodic/declarative memory and spatial navigation (OKeefe and

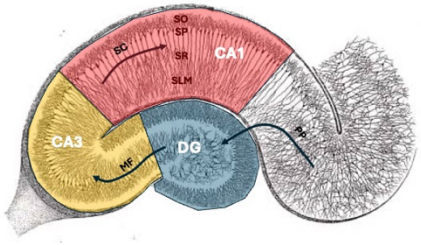

Figure 1. Organization of the hippocampal formation in a transverse slice.
The schematic shows major subfields and laminae of the hippocampus, including the dentate gyrus (DG), CA3, and CA! regions. Entorhinal cortex layer II neurons project via the perforant path (PP) to granule cells of the DG, which in turn send mossy fiber (MF) projections to CA3 pyramidal neurons. CA3 neurons project to CA1 pyramidal neurons through the Schaffer collaterals (SCs). Within CA1, distinct laminae are indicated: stratum oriens (SO), stratum pyramidale (SP), stratum radiatum (SR), and stratum lacunosum-moleculare (SLM). Together, these structures comprise the canonical tri-synaptic circuit that supports hippocampal processing.

Dostrovsky, 1971; Eichenbaum, 2017).

A key advantage for physiology is the laminar architecture of the hippocampus, which separates cell bodies, dendrites, and axons into highly organized layers: in CA1, stratum oriens (basal dendrites/ interneurons), stratum pyramidale (pyramidal somata), stratum radiatum (proximal apical dendrites and Schaffer collateral terminals), and stratum lacunosum-moleculare (distal apical tufts receiving temporo-ammonic input) (Megias et al., 2001; Spruston, 2008). This lamination preserves afferent/efferent geometry in slices, minimizes pathway mixing, and creates distinct current source sink patterns so that extracellular signals map cleanly onto underlying synaptic events (Eccles, 1979; Payne et al., 1982; Viana Di Prisco, 1984). In practice, it allows one to place a stimulating electrode squarely in the SC axon bundle and a recording electrode in stratum radiatum a few hundred microns away to capture a large, monotonic population fEPSP with minimal contamination from other pathways (Schwartzkroin and Wester, 1975). Because SC terminals are densely packed along proximal CA1 apical dendrites, one gets an excellent signal-to-noise ratio and a wide dynamic range that is ideal for measuring changes in initial slope, input–output curves, paired-pulse facilitation, and plasticity (Manabe et al., 1993).

The SC-CA1 synaptic pathway is mechanistically convenient, as its long-term potentiation (LTP) is classically N-methyl-D-aspartate receptor (NMDAR) -dependent and largely postsynaptic, allowing for direct analysis of dendritic Ca^{2+} influx, CaMKII/ PKA/ERK signaling, alpha-amino-3-hydroxy-5-methyl isoxazolepropronic acid receptor (AMPAR) trafficking, and spine-level expression mechanisms (Collingridge et al., 1983; Bliss and Collingridge, 1993; Malenka and Bear, 2004). That contrasts with DG-CA3 mossy-fiber LTP, which is strongly presynaptic and NMDAR independent, and is powerful but less aligned with the postsynaptic rules that dominate neocortical circuits (Zalutsky and Nicoll, 1990). In CA1, the clean separation of inputs by layer (SC in radiatum vs. temporoammonic in lacunosum-moleculare) allows pathway-specific stimulation and straightforward occlusion controls using two independent Schaffer inputs (Remondes and Schuman, 2002). If needed, CA3 can be removed surgically to reduce recurrent activity without disrupting the local SC termination zone, further stabilizing baseline transmission and LTP induction (Madison and Nicoll, 1984). Together, the hippocampus's ordered circuitry,

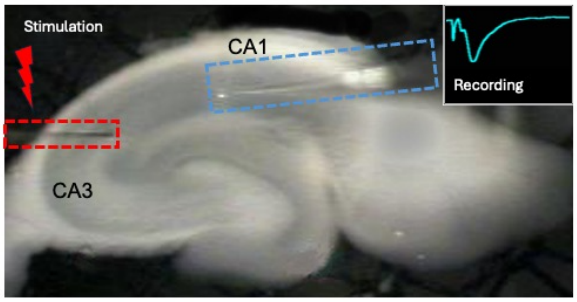

Figure 2. Photograph of a hippocampal slice positioned in an interface recording chamber.
An acute mouse hippocampal slice is shown resting on the porous membrane of the recording chamber, perfused with carbogenated ACSF at 30–32 °C. The bipolar stimulating electrode, indicated in the figure by a red dotted box, is positioned within the Schaffer collateral (SCs) pathway. The glass recording electrode (1–3 MΩ, ACSF-filled), indicated by a blue dotted box, is placed in the stratum radiatum (SR) of CA1 to capture field excitatory postsynaptic potentials (fEPSPs). A representative fEPSP trace is displayed, with the initial slope marked as the primary measure of synaptic efficacy. Strategic placement of stimulating and recording electrodes within CA1's laminar architecture enables robust, reproducible recordings with minimal pathway contamination, supporting input–output analyses, paired-pulse protocols, and long-term potentiation studies.

layered microanatomy, and the accessibility of the Schaffer collateral pathway make SC→CA1 the optimal choice for extracellular recordings of excitatory transmission and plasticity. One can stimulate a single, well-defined excitatory pathway, record a robust and lamina-locked fEPSP, and interpret changes in the initial slope as quantitative, pathway-specific shifts in synaptic strength, importantly, all with high reproducibility across slices, animals, and labs (Malenka and Bear, 2004).

Long-Term Potentiation

Long-term potentiation (LTP), first described in the 1970s, is the archetypal model for experience-dependent synaptic strengthening (Bliss and Lomo, 1973; Bliss and Richter-Levin, 1993). It refers to the persistent enhancement of synaptic efficacy following specific patterns of activity and is widely regarded as a cellular correlate of learning and memory (Malenka and Bear, 2004). The induction of LTP requires a cascade of tightly coordinated events, including presynaptic release of glutamate, postsynaptic activation of NMDA receptors, calcium entry into dendritic spines, and the engagement of intracellular signaling pathways such as CaMKII, PKA, and ERK/MAPK (Lisman et al., 2002; Sweatt, 2004). These molecular signals converge to alter AMPA receptor trafficking, modify the actin cytoskeleton, and drive gene transcription that stabilizes synaptic change (Kandel, 2001; Malinow and Malenka, 2002). In this way, LTP embodies the Hebbian principle of "cells that fire together wire together," providing a mechanistic bridge between activity patterns and enduring memory formation (Bi and Poo, 1998).

Electrophysiological field recordings in hippocampal slices have become the gold standard for studying LTP because they preserve much of the intrinsic connectivity of the circuit while permitting precise control over the extracellular environment. By recording fEPSPs in the stratum radiatum of CA1, investigators can quantify baseline synaptic strength, evaluate presynaptic release probability through paired-pulse paradigms, and induce LTP with defined stimulation protocols. This approach offers a reproducible and quantitative window into how synapses respond to activity, allowing researchers to parse contributions of specific receptors, signaling cascades, or pharmacological manipulations. Importantly, field recordings also extend beyond basic mechanistic studies, providing a powerful translational platform for modeling human neurological and neurodevelopmental disorders (NDDs). In mouse models of human NDD and neurodegenerative disorders (ND), electro-physiological assays reveal characteristic synaptic phenotypes (Jiang et al., 1998; Palop et al., 2011). For example, shifts in input–output curves can signal diminished basal transmission, while abnormalities in paired-pulse facilitation may indicate presynaptic dysfunction (Manabe et al., 1993; Zucker and Regehr, 2002). Impaired LTP magnitude under specific induction paradigms can point to deficits in postsynaptic receptor signaling or downstream kinase pathways (Bliss and Collingridge, 1993; Malenka and Bear, 2004).

Thus, the study of hippocampal CA1 field electrophysiology provides dual benefits: it deepens our understanding of the cellular mechanisms underlying learning and memory while simultaneously offering insight into how genetic or molecular perturbations disrupt synaptic function in disease states. The following is a basic procedural guide for performing hippocampal CA1 electrophysiology and reviews examples of how this technique has provided insight into the molecular mechanism and consequences of Ube3a deficiency in various mouse models of AS.

Materials and Methods for LTP

Slice Preparation

Mice or rats are rapidly decapitated, potentially under deep anesthesia, and brains are immediately placed into ice-cold, carbogenated sucrose-based cutting solution. This solution is designed to minimize excitotoxicity during slicing by replacing most sodium with sucrose and by increasing Mg^{2+} and decreasing Ca^{2+} concentrations. A typical formulation used by Sweatt and colleagues contains (in mM): 110 sucrose, 60 NaCl, 3 KCl, 26 $NaHCO_3$, 1.25 NaH_2PO_4, 7 $MgCl_2$, 0.5 $CaCl_2$, 0.6 sodium ascorbate, and 10 glucose equilibrated with 95% O_2/5% CO_2 (Levenson et al., 2002; Weeber et al., 2003; Beffert et al., 2006; Moretti et al., 2006). Using a vibrating microtome (Leica VT1000 or equivalent vibrotome), 300–400 μm transverse hippocampal slices are prepared. The chosen thickness depends on the intended recording

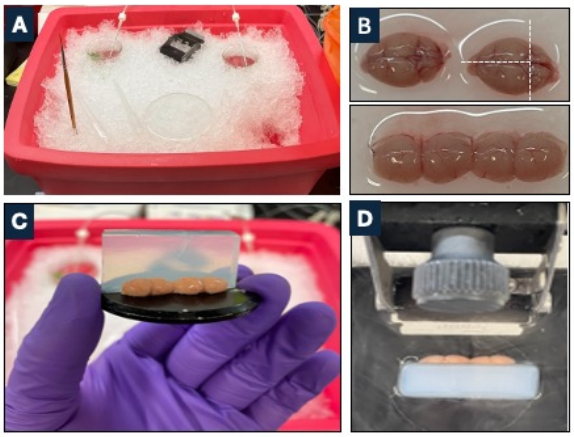

Figure 3. Preparation of acute hippocampal slices for electrophysiology.
(A) Ice bucket containing carbogenated cutting solution and transitional half cutting/half ACSF, maintained at near-ice temperature to preserve tissue viability during brain extraction and early handling. (B) Whole mouse brains immediately following dissection. The cerebellum is removed with a coronal cut just behind the inferior colliculi using a scalpel or iridectomy scissors. A sagittal cut is then made along the midline to separate the hemispheres. Each hemibrain is placed with the medial surface facing up, and the neocortex with the underlying hippocampus is separated from the midbrain and brainstem. Meninges and associated blood vessels are carefully removed to expose the hippocampus. (C) Positioning of the hemibrain on an agar block affixed to the slicing platform for stabilization during vibratome sectioning. (D) Hemibrain mounted on agar in the vibratome chamber immediately prior to slicing into 300-400 µm thick transverse sections. This stepwise preparation ensures preservation of hippocampal architecture for reliable electrophysiological recordings.

setup, as thinner slices (300 µm) are advantageous for whole-cell recordings in submersion chambers, whereas thicker slices (400 µm) are more applicable for field recordings in interface chambers (Hajos and Mody, 2009; Ting et al., 2014).

Brain Preparation

For acute slice electrophysiology, brains must be removed rapidly and with minimal disturbance to their intrinsic physiology. The standard approach is decapitation under brief isoflurane exposure or without prolonged anesthesia, followed by immediate immersion of the brain in ice-cold, carbogenated cutting solution (Ting et al., 2014). In contrast, systemic anesthesia can profoundly alter brain chemistry in ways that directly compromise electrophysiological measurements. Many anesthetics (e.g., pentobarbital, ketamine, urethane, or halothane) act on GABAA receptors, NMDA receptors, or potassium channels, which are the very targets under study in hippocampal synaptic physiology (Snyder et al., 2007; Speigel et al., 2023). Even a short exposure can change baseline excitability, suppress synaptic transmission, or modify intracellular signaling cascades such as MAPK and CaMKII. Residual drug bound to receptors in the tissue can persist after slicing, confounding results by reducing NMDA receptor responsiveness or enhancing inhibitory tone (Zorumski et al., 2016).

Moreover, anesthetics can alter neurotransmitter release, extracellular pH, and metabolic state, introducing variability in synaptic responses. For example, volatile anesthetics reduce glutamate release probability and depress hippocampal LTP induction, while barbiturates prolong inhibitory postsynaptic currents (Maclver et al., 1996; Zorumski et al., 2016). Because field electrophysiology assays rely on precise quantification of synaptic strength and plasticity, these drug-induced artifacts make it difficult to distinguish genuine disease phenotypes from anesthetic effects. Therefore, rapid decapitation, usually preceded only by minimal isoflurane to reduce distress, is the most reliable method to ensure that brain tissue reflects the animal's native physiology at the moment of euthanasia (Hajos and Mody, 2009; Ting et al., 2014). This approach preserves the integrity of synaptic currents, signaling pathways, and plasticity mechanisms, which are especially critical when comparing subtle differences between wild-type and disease model animals such as Angelman syndrome mice (Jiang et al., 1998).

ACSF Composition and Use

A precise, freshly prepared ACSF is essential for reliable fEPSP recordings because small shifts in divalent cations, pH, or osmolarity measurably change excitability, release probability, and plasticity thresholds (Hajos and Mody, 2009). ACSF needs to be prepared daily with 18 MΩ water and the exact recipe; continuously bubble with 95% O_2/5% CO_2 so the bicarbonate buffer sets pH 7.3–7.4 at the recording temperature (re-check pH after warming). To minimize loss of free Ca^{2+}/Mg^{2+} to insoluble salts, control order of addition and mixing: dissolve NaCl → KCl → glucose → $NaHCO_3$ → NaH_2PO_4 → $MgCl_2$ in ~80–90% final volume, continue carbogenation, and add $CaCl_2$ last after the solution clears and equilibrates. Avoid concentrated local contacts between $CaCl_2$ and bicarbonate or phosphate (common causes of $CaCO_3$ or $Ca_3(PO_4)_2$ precipitates); keep phosphate low (as in the recipe), maintain CO_2 in the reservoir with continuous oxygenation. Discard any solution that

turns hazy as "milky" ACSF means your free divalent levels are improper. When using drug additions, add from fresh stocks and keep vehicle (e.g., DMSO) ≤0.1% final. Be sure to protect light-sensitive antagonists (e.g., CNQX). For Mg^{2+}-free ACSF, replace $MgCl_2$ osmotically (e.g., with equimolar NaCl) and note the marked increase in network excitability. Consistency in formulation, order of addition, carbogenation, and same-day use prevents divalent precipitation and buffer drift, representing two silent failure modes that otherwise flatten slopes, shift LTP thresholds, and compromise reproducibility.

Recovery of Acute Hippocampal Slices

Recovery following slicing is a critical step in preparing acute hippocampal tissue for electrophysiological recordings. The slicing procedure itself is traumatic: axons and dendrites are severed, ionic gradients are disrupted, and cells experience transient depolarization. As a result, freshly cut slices are electrically silent and do not immediately display stable synaptic activity. A carefully staged recovery protocol is therefore essential to restore physiological function, re-establish ionic balance, and allow cells to regain excitability. The protocol typically begins with immersion of tissue in ice-cold cutting solution (Figure 3A), which reduces metabolic demand (Aghajanian et al., 1990). Importantly, cutting solution is formulated with low Ca^{2+} and high Mg^{2+} concentrations: low calcium minimizes activation of voltage-gated Ca^{2+} channels and excitatory neurotransmitter release during slicing, while high magnesium competitively blocks NMDA receptors. Together, these modifications suppress synaptic activity at the moment of tissue injury, protecting neurons from excitotoxic damage.

Once slices are sectioned, they are often transferred to a solution containing half cutting solution and half ACSF at near-ice temperature. This intermediate step allows a gradual transition between ionic environments and prevents sudden osmotic or ionic shock. Following this, slices are moved to room temperature ACSF (22–24 °C) for an extended recovery period, typically 60–90 minutes. During this phase, metabolic activity increases slightly, and neurons begin to re-establish resting potentials, synaptic vesicle cycling, and receptor function. At this stage, extracellular calcium is restored to

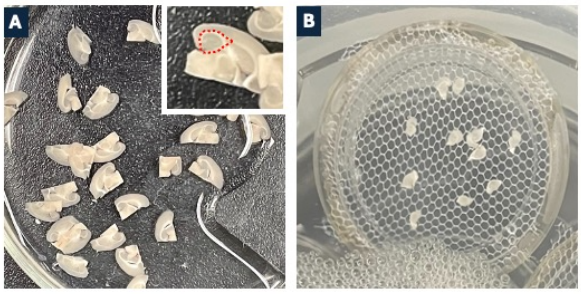

Figure 4. Dissection and placement of hippocampal slices for extracellular field recordings.
(A) Transverse 400 µm hemibrain slices collected in a chilled petri dish. Inset: schematic highlighting the region of the hemibrain slice where the hippocampal formation is dissected away from surrounding neocortex and subcortical structures, indicated with a dotted red line. (B) Isolated hippocampal slices positioned on a mesh support within an interface recording chamber. Continuous perfusion with carbogenated ACSF provides oxygenation and nutrient exchange, maintaining slice viability during extracellular field potential recordings.

physiological levels (2–2.5 mM) while magnesium is lowered to ~1 mM. Higher Ca^{2+} in ACSF is necessary for normal neurotransmitter release and postsynaptic signaling, ensuring that synaptic transmission measured during experiments reflects in vivo conditions.

The final step of recovery occurs when slices are transferred to the recording chamber warmed to 30–32 °C, where they are superfused with carbogenated ACSF (Figure 5). This gradual warming from ice-cold cutting conditions to near-physiological temperature is essential, as it allows slices to adapt to increased metabolic demands without inducing thermal stress. At this temperature range, enzymatic reactions, channel kinetics, and synaptic vesicle release nearly similar to in vivo physiology, producing stable and reproducible field potentials. Some laboratories employ interface chambers, which maximize oxygenation by exposing slices to humidified carbogen above the ACSF, whereas others use submersion chambers, where slices are continuously bathed in flowing ACSF. Both approaches have advantages; interface chambers favor robust LTP, while submerged chambers facilitate whole-cell patch recordings. In some experiments, the CA3 region is surgically removed after recovery to prevent recurrent excitatory activity from reverberating back into CA1, thereby isolating Schaffer collateral input (Madison and Nicoll, 1984). This step is particularly useful when field recordings are used to quantify long-term potentiation, as it eliminates polysynaptic contamination and ensures that evoked responses

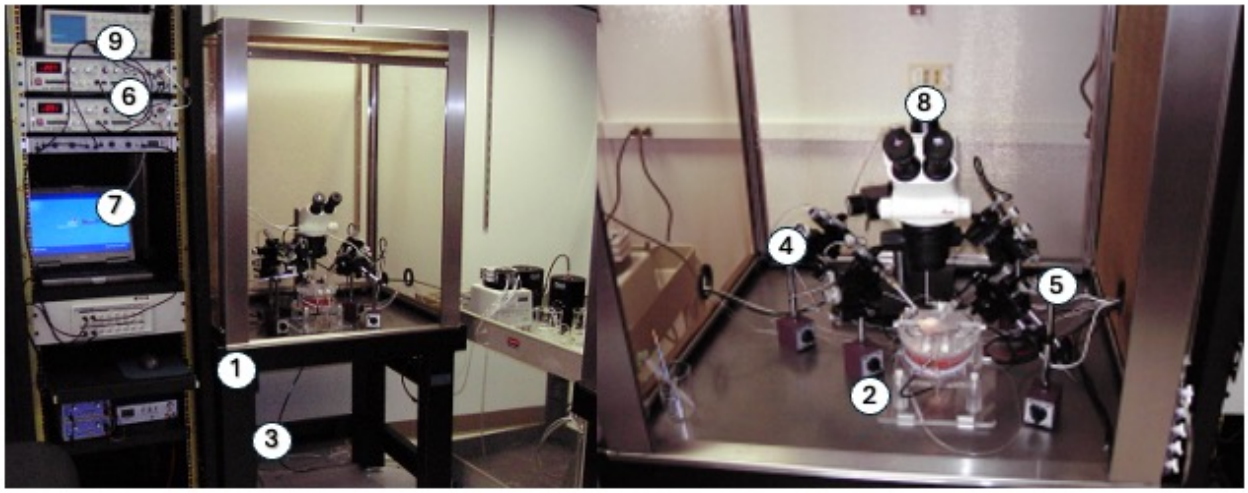

Figure 5. Extracellular field-recording rig (interface slice chamber).
Representative electrophysiology workstation for field recordings from acute brain slices in an interface chamber. The setup comprises: (1) a vibration-isolation table with an acoustic/Faraday enclosure to reduce mechanical and electrical noise; (2) an interface slice chamber (humidified, warmed) with continuous perfusion of carbogenated ACSF delivered from a reservoir via peristaltic pump, in-line bubble trap, flow meter, and in-line heater/thermistor feedback with temperature controller; (3) a stimulating electrode (e.g., bipolar Pt/Ir or tungsten) driven by a constant-current stimulus isolator receiving TTL commands from the acquisition computer; (4) a recording electrode (pulled glass micropipette, ~1–3 MΩ) mounted on a low-drift micromanipulator for positioning in the target layer (e.g., CA1 stratum radiatum) to measure extracellular fEPSPs/population spikes; (5) a headstage and differential extracellular amplifier with selectable gain and hardware filters (high-pass/low-pass), followed by a digitizer (A/D converter) connected to the control PC; (6) control and acquisition software on the computer for protocol design (input–output curves, paired-pulse, LTP/LTD), stimulus timing, and real-time display/analysis; (7) an upright microscope with low-power optics (and optional camera/IR-DIC) for slice visualization; (8) a grounding bus and shielded BNC cabling to minimize 50/60-Hz interference; (9) auxiliary devices including a gas mixer (95% O_2/5% CO_2) for ACSF oxygenation, solution pre-heater, waste collection, and power conditioning/UPS. Together, these components permit stable, low-noise extracellular recordings in interface conditions while delivering precise electrical stimulation and tightly controlled temperature, oxygenation, and flow.

represent monosynaptic CA3-CA1 transmission. This method is used, but it is not necessary for Schaefer collateral synapse recording.

Recording Setup

Slices are transferred to the recording chamber, where temperature is maintained at 30–32 °C for most field recordings or at room temperature for certain whole-cell protocols. A bipolar stimulating electrode (platinum–iridium or tungsten) is positioned in the Schaffer collateral pathway, and a glass microelectrode (1–3 MΩ) filled with ACSF is placed in the stratum radiatum of CA1 to record synaptic responses (Andersen et al., 1971; Manabe et al., 1993). Field excitatory postsynaptic potentials (fEPSPs) are evoked with test pulses delivered at 0.05 Hz, a low frequency chosen to avoid induction of synaptic plasticity during baseline acquisition (Malenka and Bear, 2004). Only slices that exhibit stable baselines, defined as less than 5% drift in fEPSP slope over a 20-minute monitoring period, are included for further analysis.

Stable baselines are essential because they ensure that subsequent changes in synaptic responses reflect genuine, stimulation-induced plasticity rather than spontaneous fluctuations in slice health or recording conditions. An unstable baseline may indicate poor slice viability, incomplete recovery of neuronal excitability, mechanical drift of the electrode, or deterioration of synaptic connections. If baseline responses are drifting upward, it could suggest pre-potentiation or spontaneous network activity that contaminates the true induction effect. Conversely, downward drift may reflect slice deterioration or loss of viable synapses. In either case, including unstable baselines would compromise the interpretation of input–output curves, paired-pulse analyses, and especially LTP experiments, where the key outcome measure is a relative increase in fEPSP slope compared to baseline. By enforcing stringent stability criteria, experimenters can confidently attribute post-stimulation changes to physiological mechanisms of plasticity rather than experimental artifacts.

Often there are challenges with maintaining a stable baseline prior to delivery of high-frequency stimulation. If fEPSP baselines drift more than 5%, several factors should be checked. First, ensure that the slice has had sufficient recovery time. Slices tested

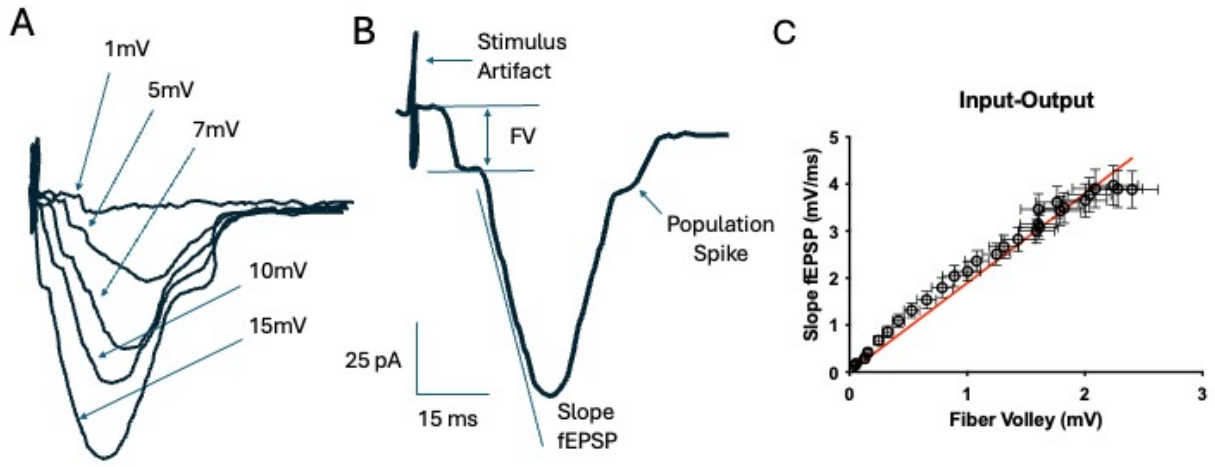

Figure 6. Theoretical input-output analysis of Schaffer collateral-CA1 synaptic responses.
(A) Example traces of field excitatory postsynaptic potentials (fEPSPs) recorded in stratum radiatum of CA1 with increasing stimulation intensities, ranging from 1 mV to 15 mV. As stimulus strength increases, both the presynaptic fiber volley and postsynaptic fEPSP slope increase in a graded manner. (B) Schematic of an individual fEPSP illustrating how the presynaptic fiber volley (initial negative deflection reflecting axonal activation) and the postsynaptic response (initial slope of the fEPSP) are measured. The fiber volley amplitude is used as an index of the number of activated presynaptic axons, while the fEPSP slope reflects the postsynaptic synaptic response. (C) Input–output curve constructed by plotting fiber volley amplitude (x-axis) against fEPSP slope (y-axis). This relationship provides a quantitative measure of synaptic gain and is commonly used to assess basal synaptic transmission, compare pre- and postsynaptic contributions, and select an appropriate stimulus intensity (typically 35–50% of maximal response) for subsequent paired-pulse and long-term potentiation experiments.

too soon after cutting often display unstable excitability. Second, confirm electrode stability: mechanical drift from vibration, perfusion turbulence, or loose micromanipulator clamping can cause artificial slope shifts. Third, evaluate perfusion flow rate and oxygenation; poor ACSF circulation or inadequate carbogenation can compromise slice viability over time. Finally, assess slice quality: pale or edematous slices are more likely to deteriorate during recording and should be excluded. Addressing these factors is critical for maintaining the fidelity of baseline recordings and ensuring reliable measures of synaptic plasticity.

Input-Output Curves

Synaptic gain is quantified by constructing input–output (I/O) curves. Stimulation intensity is systematically varied (typically 2.5–45 μA), and the slope of the fEPSP is plotted against either the applied current or the amplitude of the presynaptic fiber volley. Six sweeps per intensity are averaged to reduce variability, and the test intensity used for subsequent experiments is selected to evoke ~35–50% of the maximal fEPSP slope. This operating point ensures that responses are positioned within the dynamic range for detecting potentiation without risking ceiling effects or saturating the synapse.

The rationale for performing I/O curves is twofold. First, they provide a functional measure of basal synaptic strength as the relationship between stimulus intensity and postsynaptic response amplitude reflects how efficiently presynaptic activity is translated into postsynaptic depolarization. A rightward shift in the curve (requiring more current for the same fEPSP slope) may indicate reduced postsynaptic sensitivity, altered receptor density, or impaired excitatory drive. Conversely, an increased slope at lower intensities can suggest enhanced postsynaptic responsiveness or synaptic hyperexcitability. Second, I/O curves allow investigators to infer aspects of presynaptic function by correlating the presynaptic fiber volley amplitude (reflecting the number of activated axons) with the postsynaptic response. A reduced postsynaptic response for a given fiber volley may reflect decreased neurotransmitter release probability, impaired vesicle cycling, or postsynaptic receptor dysfunction. In contrast, a strong linear relationship between volley size and fEPSP slope suggests intact coupling between presynaptic activation, causing neurotransmitter release, and postsynaptic responsiveness. Thus, constructing I/O curves is not only a technical step for choosing an appropriate test stimulus, but it is also an essential analytic tool for detecting subtle pre- and

postsynaptic alterations in animal models of human neurological disorders.

LTP Induction Paradigms

Long-term potentiation (LTP) is induced in a threshold, nonlinear manner: weak activity yields only short-term potentiation, whereas sufficiently strong, patterned synaptic activity produces stable LTP. High-frequency stimulation (HFS) protocols are therefore used both to probe the induction threshold and, by escalating stimulus strength, to test the maximum capacity of the plasticity machinery of neurons. In hippocampal CA1, a common starting point is to set baseline test pulses at an intensity that evokes ~30–40% of the maximal fEPSP slope and then apply brief 100 Hz trains to cross the induction threshold. The 30-40% is used to preserve dynamic range of the fEPSP, avoiding ceiling effects and population spikes so that subsequent potentiation can be detected as a proportional increase in initial slope rather than saturating the input–output relation.

A widely used, "classical" HFS protocol consists of two 1 second trains at 100 Hz separated by approximately 20 seconds. In mouse CA1, this produces robust LTP that is largely extracellular signal-regulated kinase-(ERK) independent; whereas in rat CA1, the same pattern is ERK-dependent, representing an instructive species difference when interpreting signaling requirements (English and Sweatt, 1997; Selcher et al., 2002). Increasing HFS strength can be done either by adding trains or, more effectively, by spacing trains by minutes (e.g., 4×1-second 100 Hz trains, 5–10 minutes apart) to recruit cAMP/PKA-CREB signaling and protein synthesis associated with late-phase LTP (Huang and Kandel, 1994; Frey and Morris, 1997). Pattern also matters: theta-patterned paradigms, either continuous theta-frequency stimulation (~5 Hz for ~30 seconds) or theta-burst stimulation (TBS; bursts of 4 pulses at 100 Hz repeated at 5 Hz, often delivered in two to three short trains), tend to impose a stronger requirement for ERK signaling in mouse CA1 than the massed 100 Hz protocol, despite comparable pulse counts (English and Sweatt, 1997; Selcher et al., 2002).

For mechanistic dissection, our laboratory also employs "ultra-high-frequency" stimulation (uHFS; e.g., 200 Hz for 1 second, repeated three times at approximately 4-minute intervals), which can elicit LTP that is comparatively NMDA receptor–independent and more reliant on voltage-gated Ca^{2+} entry. This allows investigators to separate defects in NMDAR-gated induction from downstream expression machinery; if a preparation fails to potentiate with NMDAR-dependent HFS/TBS but responds normally to uHFS, the defect likely lies in the induction route rather than the capacity for AMPAR insertion and synaptic strengthening (Weeber et al., 2003). Critically, saturating stimulation by escalating

Paradigm	Pattern & Parameters	Mechanistic Emphasis	Species Note	Typical Use
Classical HFS	2 × 1-sec trains @ 100 Hz, 20 sec apart	NMDAR-dependent induction; postsynaptic expression	Mouse CA1 largely ERK-independent; rat CA1 ERK-dependent	Standard LTP induction and cross-species comparison
Spaced HFS (late-LTP bias)	4 × 1-sec trains @ 100 Hz, 5–10 min apart	Recruits cAMP/PKA-CREB and protein synthesis (late LTP)	As above	Tests consolidation /translation dependence
Theta-frequency stimulation (TFS)	~5 Hz continuous for ~30 sec	Stronger ERK requirement in mouse CA1	ERK-sensitive	Naturalistic pattern; tests induction pathway dependence
Theta-burst stimulation (TBS)	Bursts of 4 pulses @ 100 Hz, repeated at 5 Hz; 2–3 short trains	NMDAR-dependent; ERK-sensitive in mouse CA1	ERK-sensitive	Mimics theta-modulated bursts; efficient induction at lower total pulses
Ultra-high-frequency stimulation (uHFS)	1-sec @ 200 Hz, repeated 3 × at ~4-min intervals	Comparatively NMDA-independent; relies more on voltage-gated Ca^{2+} entry	—	Dissects induction route vs expression capacity; useful when NMDAR-dependent LTP fails

threshold-level HFS/TBS to spaced, repeated induction until additional bouts produce no further increase in fEPSP slope provides an operational readout of the network's maximum LTP capacity. This is especially informative in models with suspected plasticity deficits (e.g., Angelman syndrome, Fragile X models, or Reelin deficiency (Weeber et al., 2003; Beffert et al., 2005; Yau et al., 2016). If threshold-level protocols are impaired but saturating stimulation achieves near-wild-type potentiation, the core capacity is intact and the phenotype reflects an elevated induction threshold or altered excitability. Conversely, if potentiation remains subnormal even after saturating HFS, the ceiling itself is reduced, implicating limits in expression or metaplastic state. In practice, investigators often combine these paradigms within the same slice (with independent input pathways to verify input specificity) to map the full stimulus–response surface of LTP from threshold to ceiling.

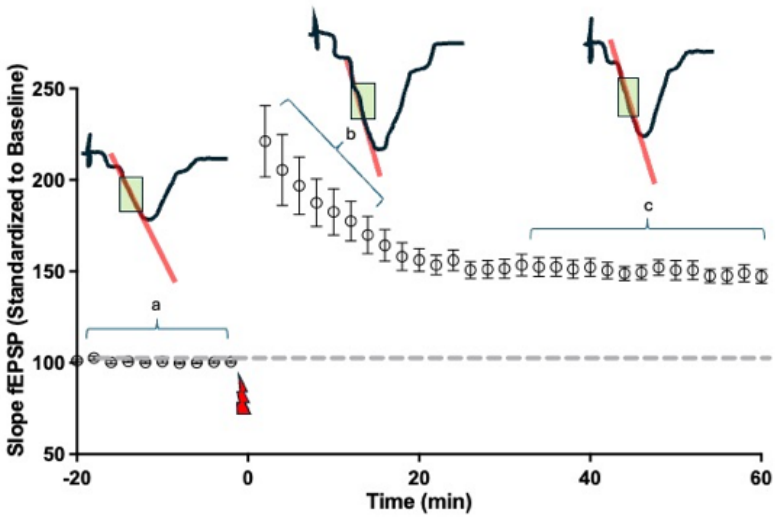

Figure 7. Example LTP experiment in hippocampal CA1.
A 20-min baseline was recorded with low-frequency test pulses, followed by delivery of high-frequency stimulation (HFS; indicated by the lightning bolt icon), and responses were monitored for 60 min post-HFS. (a) Representative baseline fEPSP; the light green box marks the fixed analysis window on the rising phase (after the fiber volley and before any population spike), and the red line indicates the linear fit used to compute the initial slope. (b) Representative fEPSP collected immediately after HFS (early post-induction), with the same analysis window and slope fit shown. (c) Representative fEPSP collected 40–60 min post-HFS (late phase), with identical window placement and slope fit. For quantification (not shown), fEPSP slopes are normalized to the mean baseline and expressed as percent of baseline; identical filtering and windowing are used across all panels. Scale bars as indicated; analysis window and slope fit are identical across a–c.

Data Acquisition and Analysis

Field EPSPs are acquired from CA1 stratum radiatum with test pulses set to evoke ~30–40% of the maximal fEPSP to avoid population spikes, digitized at 10 kHz and hardware– or software–low-pass filtered at 2 kHz (no additional smoothing), then quantified by the initial slope measured on the linear rising phase. To ensure physiological relevance and comparability, the slope is calculated with a fixed, pre-registered window positioned after the fiber volley and before any population spike. For example, a 1–2 millisecond window anchored to the end of the fiber volley or the segment spanning ~10–40% of the waveform's peak using linear regression (not peak amplitude) so that small differences in kinetics do not distort the metric. The exact placement of this window must remain identical across baseline and post-induction epochs, animals, and groups; changing the window or filter settings mid-experiment can create artifactual "plasticity." Responses are normalized to the mean baseline slope (typically the last 10–15 minutes before induction) and expressed as the percent of baseline; LTP magnitude is reported as the average potentiation over 45–60 minutes after induction, or a prespecified late window that can last up to 3 hours post tetanus (Malenka and Bear, 2004; Whitlock et al., 2006). Data quality controls are essential: maintain high SNR, stable electrode placement and stimulus intensity, and avoid over-filtering (which can blunt the rising phase and underestimate slope). Exclude datasets with unstable baselines (e.g., >5% drift or rising noise floor), movement or electrical artifacts, spontaneous or stimulus-evoked population spikes contaminating the slope window, or large fiber-volley jitter. Adhering to these acquisition and analysis conventions that require clean, minimally filtered traces, fixed, well-defined slope window, and strict stability criteria will yield robust, reproducible fEPSP measurements sensitive to true changes in synaptic strength.

Paired-Pulse Facilitation in Acute Hippocampal Slices

Paired-pulse facilitation (PPF) is a classic electrophysiological technique used to assess presynaptic function by measuring short-term plasticity of synaptic transmission. When two stimuli are delivered in rapid succession to a presynaptic input, the second postsynaptic response is typically enhanced relative to the first. This facilitation is attributed to residual calcium remaining in presynaptic terminals following the first stimulus, which increases the probability of neurotransmitter vesicle release during the second (Zucker and Regehr, 2002). Importantly, PPF provides insight into presynaptic release probability, complementing information obtained from input–output (I/O) experiments. While I/O curves characterize postsynaptic responsiveness to varying stimulus strengths, PPF directly probes the dynamics of neurotransmitter release. Combining these approaches enables investigators to parse presynaptic versus postsynaptic contributions to synaptic function, thereby producing a more complete understanding of circuit physiology. For example, a slice showing a steep I/O relationship but reduced PPF may indicate high postsynaptic sensitivity coupled with high presynaptic release probability, whereas the opposite pattern may suggest reduced release probability as a limiting factor.

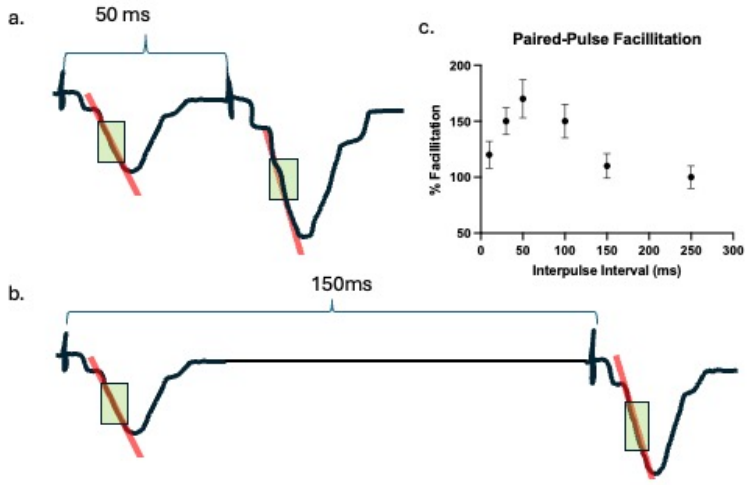

Figure 8. Paired-pulse facilitation (PPF) at Schaffer collateral-CA1 synapses.
(a) Representative field excitatory postsynaptic potentials (fEPSPs) evoked by two stimuli delivered at a 30 ms interpulse interval (IPI). The second fEPSP exhibits a steeper initial slope compared to the first (green box highlights the slope measurement region; red line indicates slope calculation).
(b) Representative fEPSPs recorded with a 150 ms IPI, showing a reduced facilitation of the second response relative to the first.
(c) Summary input–output graph of theoretical paired-pulse ratios (PPR, $slope_2/slope_1 \times 100\%$) across multiple IPIs (10, 30, 50, 100, and 150 ms). The curve illustrates the expected decay of facilitation as the IPI increases, reflecting presynaptic release probability and short-term synaptic dynamics in CA1 hippocampal circuits.

To elicit PPF, two identical stimuli are delivered at a fixed intensity, commonly set to evoke 30–40% of the maximal fEPSP slope. Interpulse intervals ranging from 20–250 milliseconds are applied, with shorter intervals (20–50 ms) producing more pronounced facilitation due to greater residual calcium accumulation. The paired-pulse ratio (PPR) is calculated by dividing the slope of the second fEPSP by the slope of the first. Repeating this procedure across several interpulse intervals generates a facilitation curve that reflects synaptic release probability.

By incorporating I/O curves into the same experimental paradigm, researchers can better contextualize PPF findings. For instance, if I/O experiments reveal altered postsynaptic responsiveness but PPF ratios remain unchanged, the underlying deficit is more likely postsynaptic. Conversely, changes in both I/O slopes and PPF may indicate combined presynaptic and postsynaptic dysfunction. This dual assessment strengthens the interpretive power of hippocampal field recordings and provides a robust framework for dissecting the mechanisms underlying synaptic transmission and plasticity. Paired-pulse facilitation (PPF) is a short-term form of synaptic plasticity that reflects presynaptic release probability.

Discussion

The maternal Ube3a null mouse ($Ube3a^{m-/p+}$), first reported by Jiang et al. (1998), has consistently shown impaired hippocampus-dependent learning accompanied by blunted CA1 LTP, cementing SC-CA1 synapses as a core electrophysiological readout of the disorder (Jiang et al., 1998; Miura et al., 2002; Jiang et al., 2010; Silva-Santos et al., 2015; Judson et al., 2016; Dodge et al., 2020; Lee et al., 2023). Importantly, mechanistic work has linked LTP deficits

to altered calcium/calmodulin-dependent protein kinase II (CaMKII) signaling: Ube3a loss impairs experience-dependent autophosphorylation of CaMKII at threonine-286, which is required for stable synaptic potentiation (Weeber et al., 2003; van Woerden et al., 2007). This disrupted coupling between N-methyl-D-aspartate receptor (NMDAR) activation and downstream kinase signaling suggests that UBE3A deficiency primarily raises the threshold for LTP induction, rendering weak or moderate stimulation insufficient to trigger long-lasting potentiation. However, in some experimental contexts, more robust induction protocols such as multiple trains of 100 Hz HFS or pharmacological disinhibition with GABA receptor antagonists (Cecere et al., 2025) can restore LTP toward wild-type levels. These findings imply that the fundamental capacity for synaptic strengthening remains intact, but access to that capacity is limited by heightened inhibitory tone or impaired NMDAR–CaMKII coupling. By contrast, other studies demonstrate that even saturating LTP protocols fail to normalize potentiation, indicating that downstream expression mechanisms, such as AMPA receptor trafficking, actin cytoskeletal remodeling, or mTORC1-dependent translational regulation, may be intrinsically disrupted (Sun et al., 2016).

Saturating long-term potentiation (LTP) paradigms provide critical insight into the distinction between synaptic induction threshold and maximum plasticity capacity in hippocampal CA1 circuits. By progressively escalating stimulation intensity, via multiple trains of high-frequency stimulation (HFS) at 100 Hz or repeated theta-burst stimulation (TBS), investigators can drive the system toward a saturation point, beyond which additional stimulation produces minimal further increases in the field excitatory postsynaptic potential (fEPSP) slope, typically plateauing at a 5–10% gain. Studies in Ube3a maternal-null (m−/p+) mice have revealed two distinct patterns. In some cases, weak or near-threshold protocols fail to induce stable potentiation, or the potentiation decays rapidly, yet robust plasticity can still be achieved with stronger or pharmacologically facilitated stimulation. This suggests that Ube3a deficiency primarily elevates the induction threshold rather than constraining the ultimate capacity for LTP. Such findings are consistent with reports of reduced NMDA receptor function, impaired NMDAR–CaMKII coupling and altered inhibitory tone in AS models (Miura et al., 2002; Weeber et al., 2003; Judson et al., 2016).

Conversely, other studies have demonstrated that even under saturating HFS or repeated TBS, the maximum potentiation achieved in Ube3a-deficient mice remains below wild-type levels. This “true ceiling” effect points toward deficits in expression or maintenance mechanisms, such as impaired AMPA receptor trafficking, actin cytoskeletal remodeling, or dysregulated translational control pathways like mTORC1, which can be corrected only through direct molecular interventions such as Ube3a reinstatement or pathway modulation (Silva-Santos et al., 2015; Lee et al., 2023). However, LTP magnitude is strongly influenced by experimental parameters, including slice preparation, recording temperature, and stimulus intensity (as described above). Variability in fiber volley recruitment across preparations can obscure whether differences reflect a genuine reduction in the maximum expression capacity of synaptic potentiation or simply reduced input–output coupling under specific conditions. Without rigorous normalization to presynaptic drive (e.g., fiber volley amplitude) and control for slice health, apparent “ceiling” differences may instead represent threshold-related impairments in induction. Furthermore, the canonical LTP paradigms used, such as saturating 100 Hz HFS or multiple-train TBS, rely heavily on NMDA receptor activation and CaMKII autophosphorylation, and reduced LTP in these contexts may not unequivocally indicate an intrinsic limit in plasticity expression capacity, but rather reflect an impaired ability to engage induction mechanisms.

Beyond revealing the parameters of induction and ceiling, saturating LTP experiments in AS mouse and rat models have provided a framework for dissecting the mechanistic underpinnings of synaptic dysfunction. Evidence from the Ube3a deletion rat model indicates comparable deficits in hippocampal plasticity, reinforcing the cross-species validity of the threshold-versus-capacity framework (Berg et al., 2020; Dodge et al., 2020). Together, these findings demonstrate that using multiple LTP paradigms can move beyond simply confirming impaired plasticity to provide a mechanistic resolution, distinguishing between deficits in induction versus expression. This mechanistic insight is essential for guiding therapeutic

strategies for AS. In particular, interventions that enhance excitatory drive or reduce inhibition may overcome elevated thresholds, while approaches targeting translational or structural pathways, or reactivating the paternal allele, may be necessary to restore the full capacity for long-term synaptic strengthening.

Acknowledgements

The authors wish to thank Dr. Kelly Knee for editing and insight.

References

Aghajanian GK, Sprouse JS, Sheldon P, Rasmussen K (1990) Electrophysiology of the central serotonin system: receptor subtypes and transducer mechanisms. Ann N Y Acad Sci 600:93-103; discussion 103.

Amaral DG, Scharfman HE, Lavenex P (2007) The dentate gyrus: fundamental neuroanatomical organization (dentate gyrus for dummies). Prog Brain Res 163:3-22.

Beffert U, Durudas A, Weeber EJ, Stolt PC, Giehl KM, Sweatt JD, Hammer RE, Herz J (2006) Functional dissection of Reelin signaling by site-directed disruption of Disabled-1 adaptor binding to apolipoprotein E receptor 2: distinct roles in development and synaptic plasticity. J Neurosci 26:2041-2052.

Beffert U, Weeber EJ, Durudas A, Qiu S, Masiulis I, Sweatt JD, Li WP, Adelmann G, Frotscher M, Hammer RE, Herz J (2005) Modulation of synaptic plasticity and memory by Reelin involves differential splicing of the lipoprotein receptor Apoer2. Neuron 47:567-579.

Berg EL et al. (2020) Translational outcomes in a full gene deletion of ubiquitin protein ligase E3A rat model of Angelman syndrome. Transl Psychiatry 10:39.

Bi GQ, Poo MM (1998) Synaptic modifications in cultured hippocampal neurons: dependence on spike timing, synaptic strength, and postsynaptic cell type. J Neurosci 18:10464-10472.

Bliss TV, Lomo T (1973) Long-lasting potentiation of synaptic transmission in the dentate area of the anaesthetized rabbit following stimulation of the perforant path. J Physiol 232:331-356.

Bliss TV, Richter-Levin G (1993) Spatial learning and the saturation of long-term potentiation. Hippocampus 3:123-125.

Bliss TV, Collingridge GL (1993) A synaptic model of memory: long-term potentiation in the hippocampus. Nature 361:31-39.

Cecere G et al. (2025) Preclinical pharmacology of alogabat: a novel GABA(A)-alpha5 positive allosteric modulator targeting neurodevelopmental disorders with impaired GABA(A) signaling. Front Pharmacol 16:1626078.

Collingridge GL, Kehl SJ, McLennan H (1983) Excitatory amino acids in synaptic transmission in the Schaffer collateral-commissural pathway of the rat hippocampus. J Physiol 334:33-46.

Dodge A, Peters MM, Greene HE, Dietrick C, Botelho R, Chung D, Willman J, Nenninger AW, Ciarlone S, Kamath SG, Houdek P, Sumova A, Anderson AE, Dindot SV, Berg EL, O'Geen H, Segal DJ, Silverman JL, Weeber EJ, Nash KR (2020) Generation of a Novel Rat Model of Angelman Syndrome with a Complete Ube3a Gene Deletion. Autism Res 13:397-409.

Eccles JC (1979) Hippocampal plasticity. Prog Brain Res 51:133-138.

Eichenbaum H (2017) The role of the hippocampus in navigation is memory. J Neurophysiol 117:1785-1796.

English JD, Sweatt JD (1997) A requirement for the mitogen-activated protein kinase cascade in hippocampal long term potentiation. J Biol Chem 272:19103-19106.

Frey U, Morris RG (1997) Synaptic tagging and long-term potentiation. Nature 385:533-536.

Hajos N, Mody I (2009) Establishing a physiological environment for visualized in vitro brain slice recordings by increasing oxygen supply and modifying aCSF content. J Neurosci Methods 183:107-113.

Huang YY, Kandel ER (1994) Recruitment of long-lasting and protein kinase A-dependent long-term potentiation in the CA1 region of hippocampus requires repeated tetanization. Learn Mem 1:74-82.

Jiang YH, Armstrong D, Albrecht U, Atkins CM, Noebels JL, Eichele G, Sweatt JD, Beaudet AL (1998) Mutation of the Angelman ubiquitin ligase in mice causes increased cytoplasmic p53

and deficits of contextual learning and long-term potentiation. Neuron 21:799-811.

Jiang YH, Pan Y, Zhu L, Landa L, Yoo J, Spencer C, Lorenzo I, Brilliant M, Noebels J, Beaudet AL (2010) Altered ultrasonic vocalization and impaired learning and memory in Angelman syndrome mouse model with a large maternal deletion from Ube3a to Gabrb3. PLoS One 5:e12278.

Judson MC, Wallace ML, Sidorov MS, Burette AC, Gu B, van Woerden GM, King IF, Han JE, Zylka MJ, Elgersma Y, Weinberg RJ, Philpot BD (2016) GABAergic Neuron-Specific Loss of Ube3a Causes Angelman Syndrome-Like EEG Abnormalities and Enhances Seizure Susceptibility. Neuron 90:56-69.

Kandel ER (2001) The molecular biology of memory storage: a dialog between genes and synapses. Biosci Rep 21:565-611.

Lee D, Chen W, Kaku HN, Zhuo X, Chao ES, Soriano A, Kuncheria A, Flores S, Kim JH, Rivera A, Rigo F, Jafar-Nejad P, Beaudet AL, Caudill MS, Xue M (2023) Antisense oligonucleotide therapy rescues disturbed brain rhythms and sleep in juvenile and adult mouse models of Angelman syndrome. Elife 12.

Levenson J, Weeber E, Selcher JC, Kategaya LS, Sweatt JD, Eskin A (2002) Long-term potentiation and contextual fear conditioning increase neuronal glutamate uptake. Nat Neurosci 5:155-161.

Lisman J, Schulman H, Cline H (2002) The molecular basis of CaMKII function in synaptic and behavioural memory. Nat Rev Neurosci 3:175-190.

Maclver MB, Mikulec AA, Amagasu SM, Monroe FA (1996) Volatile anesthetics depress glutamate transmission via presynaptic actions. Anesthesiology 85:823-834.

Madison DV, Nicoll RA (1984) Control of the repetitive discharge of rat CA 1 pyramidal neurones in vitro. J Physiol 354:319-331.

Malenka RC, Bear MF (2004) LTP and LTD: an embarrassment of riches. Neuron 44:5-21.

Malinow R, Malenka RC (2002) AMPA receptor trafficking and synaptic plasticity. Annu Rev Neurosci 25:103-126.

Manabe T, Wyllie DJ, Perkel DJ, Nicoll RA (1993) Modulation of synaptic transmission and long-term potentiation: effects on paired pulse facilitation and EPSC variance in the CA1 region of the hippocampus. J Neurophysiol 70:1451-1459.

Megias M, Emri Z, Freund TF, Gulyas AI (2001) Total number and distribution of inhibitory and excitatory synapses on hippocampal CA1 pyramidal cells. Neuroscience 102:527-540.

Miura K, Kishino T, Li E, Webber H, Dikkes P, Holmes GL, Wagstaff J (2002) Neurobehavioral and electroencephalographic abnormalities in Ube3a maternal-deficient mice. Neurobiol Dis 9:149-159.

Moretti P, Levenson JM, Battaglia F, Atkinson R, Teague R, Antalffy B, Armstrong D, Arancio O, Sweatt JD, Zoghbi HY (2006) Learning and memory and synaptic plasticity are impaired in a mouse model of Rett syndrome. J Neurosci 26:319-327.

O'Keefe J, Dostrovsky J (1971) The hippocampus as a spatial map. Preliminary evidence from unit activity in the freely-moving rat. Brain Res 34:171-175.

Palop JJ, Mucke L, Roberson ED (2011) Quantifying biomarkers of cognitive dysfunction and neuronal network hyperexcitability in mouse models of Alzheimer's disease: depletion of calcium-dependent proteins and inhibitory hippocampal remodeling. Methods Mol Biol 670:245-262.

Payne K, Wilson CJ, Young S, Fifkova E, Groves PM (1982) Evoked potentials and long-term potentiation in the mouse dentate gyrus after stimulation of the entorhinal cortex. Exp Neurol 75:134-148.

Remondes M, Schuman EM (2002) Direct cortical input modulates plasticity and spiking in CA1 pyramidal neurons. Nature 416:736-740.

Schwartzkroin PA, Wester K (1975) Long-lasting facilitation of a synaptic potential following tetanization in the in vitro hippocampal slice. Brain Res 89:107-119.

Selcher JC, Weeber EJ, Varga AW, Sweatt JD, Swank M (2002) Protein kinase signal transduction cascades in mammalian associative conditioning. Neuroscientist 8:122-131.

Silva-Santos S, van Woerden GM, Bruinsma

CF, Mientjes E, Jolfaei MA, Distel B, Kushner SA, Elgersma Y (2015) Ube3a reinstatement identifies distinct developmental windows in a murine Angelman syndrome model. J Clin Invest 125:2069-2076.

Snyder GL, Galdi S, Hendrick JP, Hemmings HC, Jr. (2007) General anesthetics selectively modulate glutamatergic and dopaminergic signaling via site-specific phosphorylation in vivo. Neuropharmacology 53:619-630.

Speigel I, Patel K, Osman V, Hemmings HC, Jr. (2023) Volatile anesthetics inhibit presynaptic cGMP signaling to depress presynaptic excitability in rat hippocampal neurons. Neuropharmacology 240:109705.

Spruston N (2008) Pyramidal neurons: dendritic structure and synaptic integration. Nat Rev Neurosci 9:206-221.

Sun J, Liu Y, Tran J, O'Neal P, Baudry M, Bi X (2016) mTORC1-S6K1 inhibition or mTORC2 activation improves hippocampal synaptic plasticity and learning in Angelman syndrome mice. Cell Mol Life Sci 73:4303-4314.

Sweatt JD (2004) Mitogen-activated protein kinases in synaptic plasticity and memory. Curr Opin Neurobiol 14:311-317.

Ting JT, Daigle TL, Chen Q, Feng G (2014) Acute brain slice methods for adult and aging animals: application of targeted patch clamp analysis and optogenetics. Methods Mol Biol 1183:221-242.

van Woerden GM, Harris KD, Hojjati MR, Gustin RM, Qiu S, de Avila Freire R, Jiang YH, Elgersma Y, Weeber EJ (2007) Rescue of neurological deficits in a mouse model for Angelman syndrome by reduction of alphaCaMKII inhibitory phosphorylation. Nat Neurosci 10:280-282.

Viana Di Prisco G (1984) Hebb synaptic plasticity. Prog Neurobiol 22:89-102.

Weeber EJ, Jiang YH, Elgersma Y, Varga AW, Carrasquillo Y, Brown SE, Christian JM, Mirnikjoo B, Silva A, Beaudet AL, Sweatt JD (2003) Derangements of hippocampal calcium/calmodulin-dependent protein kinase II in a mouse model for Angelman mental retardation syndrome. J Neurosci 23:2634-2644.

Whitlock JR, Heynen AJ, Shuler MG, Bear MF (2006) Learning induces long-term potentiation in the hippocampus. Science 313:1093-1097.

Witter MP (2007) Intrinsic and extrinsic wiring of CA3: indications for connectional heterogeneity. Learn Mem 14:705-713.

Yau SY, Bostrom CA, Chiu J, Fontaine CJ, Sawchuk S, Meconi A, Wortman RC, Truesdell E, Truesdell A, Chiu C, Hryciw BN, Eadie BD, Ghilan M, Christie BR (2016) Impaired bidirectional NMDA receptor dependent synaptic plasticity in the dentate gyrus of adult female Fmr1 heterozygous knockout mice. Neurobiol Dis 96:261-270.

Zalutsky RA, Nicoll RA (1990) Comparison of t wo forms of long-term potentiation in single hippocampal neurons. Science 248:1619-1624.

Zorumski CF, Izumi Y, Mennerick S (2016) Ketamine: NMDA Receptors and Beyond. J Neurosci 36:11158-11164.

Zucker RS, Regehr WG (2002) Short-term synaptic plasticity. Annu Rev Physiol 64:355-405.